



Thiabendazole/bentonites hybrids as controlled release systems

Graycyelle R.S. Cavalcanti, Maria G. Fonseca, Edson da Silva Filho, Maguy Jaber

► To cite this version:

Graycyelle R.S. Cavalcanti, Maria G. Fonseca, Edson da Silva Filho, Maguy Jaber. Thiabendazole/bentonites hybrids as controlled release systems. *Colloids and Surfaces B: Biointerfaces*, 2019, 176, pp.249-255. 10.1016/j.colsurfb.2018.12.030 . hal-02169301

HAL Id: hal-02169301

<https://hal.sorbonne-universite.fr/hal-02169301>

Submitted on 1 Jul 2019

HAL is a multi-disciplinary open access archive for the deposit and dissemination of scientific research documents, whether they are published or not. The documents may come from teaching and research institutions in France or abroad, or from public or private research centers.

L'archive ouverte pluridisciplinaire **HAL**, est destinée au dépôt et à la diffusion de documents scientifiques de niveau recherche, publiés ou non, émanant des établissements d'enseignement et de recherche français ou étrangers, des laboratoires publics ou privés.

Thiabendazole/bentonites hybrids as controlled release systems

Graycyelle R. S. Cavalcanti^{1,3}, Maria G. Fonseca^{1*}, Edson C. da Silva Filho² and Maguy Jaber^{*3}

¹*Núcleo de Pesquisa e Extensão - Laboratório de Combustíveis e Materiais (NPE - LACOM). Universidade Federal da Paraíba, Cidade Universitária, s/n - Castelo Branco III, 58051-085, João Pessoa - PB, Brazil.*

²*Interdisciplinary Laboratory of Advanced Materials, CCN, UFPI, 64049-550, Teresina, Piauí, Brazil,*

³*Sorbonne Université, Laboratoire d'Archéologie Moléculaire et Structurale, CNRS UMR 8220, Tour 23, 3ème étage, couloir 23-33, BP 225, 4 place Jussieu, 75005 Paris, France.*

The manuscript includes 4432 words, 6 figures and 2 tables

Highlights

- Thiabendazole intercalates in the interlamellar space of bentonite.
- The nature of the interlamellar cation influenced the adsorption capacity of bentonite.
- Release tests showed that part of the drugs are still adsorbed on the bentonites.
- The solids have shown to be promising for pharmaceutical applications.

Abstract

Clay minerals are commonly used in pharmaceutical products as excipients and active agents. New drug vehicles based on clay minerals have been developed. In this work, sodium (BentNa), calcium (BentCa) and magnesium (BentMg) exchanged bentonites were used for the sorption of thiabendazole (TBZ), and their potential use as controlled release systems was evaluated. Pristine bentonite and exchanged bentonites were characterized by X-ray diffraction, infrared spectroscopy, thermogravimetry and transmission electron microscopy (TEM), and the influence of the different parameters such as pH, contact time and initial concentration of the drug was investigated. The maximum adsorption reached after 45 min period with 2000 mg L⁻¹ of thiabendazole to BentNa and after 105 min with 1300 mg L⁻¹ to BentCa and BentMg, respectively. The maximum adsorbed quantities of thiabendazole were 164.4; 152.3 and 133.3 mg g⁻¹ for BentNa, BentCa and BentMg, respectively. The emission profiles obtained for the bentonite/drug hybrids were similar when simulated body fluids were used and these emission profiles were fitted according to the Korsmeyer-Peppas kinetic model.

Keywords: *Clay minerals, Drug delivery system, thiabendazole, clay/drugs hybrids*

The manuscript includes 4432 words, 6 figures and 2 tables

1. Introduction

Clay minerals are an important class of natural materials which are used in traditional medicine [1], their biological uses having been reported since antiquity. The medicinal properties of clay minerals have long been recognized in indigenous cultures, and their use in traditional medicine confined mainly to external applications for the treatment of skin problems and gastrointestinal diseases [2].

The specific physical and chemical properties of clay minerals such as adsorption, cation exchange capacity, swelling capacity, ability to form colloidal solutions, optimum rheological behavior and dispersibility in water [3-6] as also their low cost, abundance, biocompatibility versatility and effectiveness, have resulted, in recent decades, in the introduction of these minerals, into various technological processes [7-16] Clay minerals have therefore now been introduced as components in various pharmacological formulations, in which they are used as excipients. In addition to classic pharmaceutical uses, they can also be employed in the development of new drug delivery systems (DDS) [17-19]

Although all pharmaceutical dosage forms can be considered to DDS (since they use the administration of drugs intended to reach a site of action and maintain a certain concentration over the entire period of treatment), the final therapeutic effect of a pharmaceutical treatment will depend on several factors, which will involve the nature of the drug as well as the form taken for its administration and dosage [2,18]. Thus, the development of new technologies which aim to reduce the quantity of the administered dose and decrease the levels of drug toxicity, has led to new controlled release systems [20].

The formation of drug/clay mineral hybrids can influence the bioavailability of the drug, the release rate, and the chemical stability of the systems [17]. For example, stronger drug/bentonite interactions resulted in slower release and lower rates of drug absorption and, in consequence, the reduction of the plasma concentration of the drug [2,21]. These properties are not desirable for drugs such as antihistamines, which require an immediate therapeutic concentration in the blood. Clay minerals are however highly recommended as carriers for drugs that require slow and prolonged release, such as antibiotics (amoxicillin, tetracycline, cephradine, metronidazole and gentamicin), antihypertensive drugs (propranolol, nifedipine, amlodipine, etc.) and antipsychotics (aripiprazole, buspirone) [22]. Thiabendazole (TBZ) is an anthelmintic and antifungal drug used in the treatment of fungal and worm infections in animals and humans [23].

Four different TBZ species can be generated by protonation–deprotonation reactions depending on the pH of the solution [24].

Previous studies have studied the adsorption of TBZ on Argentine clay, [25,26]. It was observed that there was a drastic reduction in TBZ adsorption when the pH was changed from 5 to 7, as a result of the presence of uncharged thiabendazole species. Moreover, at a pH lower than 2, the ion exchange is the main mechanism of adsorption. Aluminum pillared montmorillonite was also used as a TBZ adsorbent in an aqueous medium [23,24].

The use of bentonite and thiabendazole for the development of controlled release systems has also been reported; Yasser (2014) used Ca-Bentonite in controlled release formulation of TBZ for reduced contaminations to soil water. Results showed that TBZ was better adsorbed in clay at the value pH 3 and the release experiments showed that liberation the TBZ that slower at pH 3 than at pH 5.5 or pH 9.

This present work focused on the study of the thiabendazole/bentonites system for drug delivery, the aim being the investigation of the influence of the interlayer cations of bentonite on the interaction with thiabendazole. The kinetics of *in vitro* release of thiabendazole from hybrids in simulated gastric (SGF), body (SBF) and intestinal (SIF) fluids were also determined.

2. Experimental

2.1 Material and chemicals

The bentonite sample was donated by the Bentonisa do Nordeste SA in Brazil (Boa Vista, PB).. The sample presented a cationic exchange capacity (CEC) of 88 cmol (+) Kg⁻¹ and the following chemical composition - SiO₂ (52.98%), Al₂O₃ (18.35 %), Fe₂O₃ (3.96%), MgO (2.47%), Na₂O (2.56%), K₂O (0.22%), with a loss ignition of 18.59%.

Thiabendazole (2-(thiazol-4-yl) benzimidazole, M = 201.3 gmol⁻¹, pKa 2.5, 4.7 and 12.0), was acquired from Sigma-Aldrich, (99% analytical grade). Thiabendazole is partially soluble in water (28 mg L⁻¹) and soluble in acid solutions at low concentrations; [23, 25, 26], a solution of the drug was therefore prepared with 3000 mg L⁻¹ drug solution in 0.01 mol L⁻¹ HCl. All the samples prepared were dried at 343 K for 48 h and then conducted for characterization.

2.2 Ion exchange

Raw bentonite (Bent) was purified to remove quartz by the centrifugation decantation method. The sample was suspended in 1.0 mol L⁻¹ NaCl, CaCl₂·2H₂O or MgCl₂·6H₂O solutions, and was maintained under orbital agitation at 300 K. The same procedure was repeated twice to guarantee the process of ion exchange [3]. The exchange samples were named BentNa, BentCa and BentMg.

2.3 Sorption of thiabendazole

We first monitored the influence of pH on the drug-bentonites interaction. Samples of 200 mg of each exchange solid was suspended in 50.0 mL of 500 mg L⁻¹ drug solution, and the pH was adjusted to 1.4, 2.3 and 3.8, the values of which were determined based on the pK_a of thiabendazole. The suspension was stirred for a period of 24 h. The final solids were centrifuged, and the thiabendazole in equilibrium solution was quantified by UV-Vis molecular spectrometry in an UV-Vis spectrophotometer Shimadzu model 2550, at 298 nm in the concentration range of 2 – 8 mg L⁻¹.

The sorbed drug on solid (q_e) was calculated by equation (1).

$$q_e = \frac{(C_0 - C_e)V}{m} \quad (1)$$

Where C_0 and C_e are the drug concentration (mg L⁻¹) in solution before and after sorption respectively, V (L) is the volume of the drug solution, and m (g) is the mass of the bentonite.

To investigate the influence of time on adsorption, the same procedure was used, and the time was varied between 0 and 120 min in the same conditions.

The effect of the initial concentration of the drug was monitored by using thiabendazole at 30 and 3000 mg L⁻¹, which reacted with bentonites at optimum conditions for both pH and time.

2.4. Synthesis of bentonite/drug hybrids

The synthesis of the hybrids was carried out basing oneself on the previous conditions of pH, time and drug concentration, as determined in the adsorption tests. Therefore, a 1.0 g sample of each bentonite category was suspended in 250 mL of 2000 mg L⁻¹ drug solution, and then reacted for a period of 45 min in the case of the sodium

bentonite, and for the calcium and magnesium samples, 1.0 g of each solid was reacted with the 1300 mgL⁻¹ drug solution for 105 min. The systems were maintained under orbital agitation at 300 K. Finally, the drug concentration was determined as described above.

2.5. Release test

For the release test, simulated gastric (SGF, HCl aqueous solution, pH 1.2), body (SBF, pH 7.4) and intestinal (SIF, phosphate buffer solution, pH 7.4) fluids were prepared. The SBF was prepared by dissolving the following chemical reagents in 1.0 L distilled water: NaCl (7.996 g), NaHCO₃ (0.350 g), KCl (0.224 g), K₂HPO₄·3H₂O (0.228 g), MgCl₂·6H₂O (0.305 g), CaCl₂ (0.278 g), Na₂SO₄ (0.071 g), NH₂C(CH₂OH)₃ (6.057 g) [27].

The release test followed standard procedure where 0.1 g of each solid BentNaTBZ, BentCaTBZ and BentMgTBZ was suspended as a disk in 400 cm³ of each fluid. The system was maintained at 335 K for 72 h, and at each time interval, aliquots of 5.0 mL of the solution were removed, and the same volume of drug solution then added to the suspension [28].

The drug concentration was quantified as described above. The cumulative drug concentration was calculated (C_c) as determined in Equation (2), where C_f (mg L⁻¹) is the final drug concentration in solution, V_f and V_a (L) are the volumes of fluid and aliquota, respectively.

$$C_c = C_f + \frac{(V_a * C_f)}{V_f} \quad (2)$$

3. Results and discussion

3.1 Characterization of exchanged bentonites

For raw bentonite, the XRD patterns of the samples (SM1) exhibited the principal montmorillonite reflection at 2θ 7.24° (d_{001} = 1.22 nm) [30]. Other reflections were observed at 2θ 19.8°; 28.5°; 34.9° and 61.8° and were indexed to montmorillonite phase in agreement with ICDD file 00-060-0318. The additional peaks at 2θ 11.7° and

26.5° were associated to muscovite and quartz phases, respectively. After removal of the quartz, the XRD patterns maintained the reflections of montmorillonite, and the quartz peaks were not observed.

After ion exchange, the samples displayed reflections at 7.55°, 6.19° and 6.17° associated to the (001) plan with basal spacings of 1.17, 1.43 and 1.43 nm for BentNa, BentMg and BentCa respectively. These values are in agreement with those observed for natural sodium [30], calcium [31] and magnesium montmorillonites [32]. In the Bent and BentNa samples, an additional peak at 28.4° is attributed to the presence of residual NaCl in according ICDD file 01-083-1728. The higher values of the basal spacings were those obtained for samples with higher hydration cation volume, 156.7 and 176.9 cm³ mol⁻¹ for Ca²⁺ and Mg²⁺, and 109.0 cm³ mol⁻¹ for Na⁺.

FTIR spectra (Figure 1ii) for all samples displayed bands at 3634 cm⁻¹, assigned to structural OH stretching (M-OH, M = Al³⁺, Mg²⁺, Fe³⁺), and at 3400 cm⁻¹ resulting from OH stretching of interlayer water and silanol (Si-OH); the OH stretching of water, however, showed a small variation which can be related to the interlayer cation. The band associated to the bending of water was observed at 1642 cm⁻¹ [33, 34]. Other bands were detected at 1121 and 1040 cm⁻¹ and assigned to Si-O assymetric and symmetric stretchings, respectively. Si-O-Al and Si-O-Si bending vibrations, were detected at 523 and 461 cm⁻¹ respectively. Isomorphic substitution of Al³⁺ for Mg²⁺ and Fe²⁺ in the octahedral sheet provokes changes in the OH deformation bands at 918 cm⁻¹ (Al-Al-OH), 876 cm⁻¹ (Al-Fe-OH) and 830 cm⁻¹ (Al-Mg-OH), and these were dependent on the nature of the cation present [35,36].

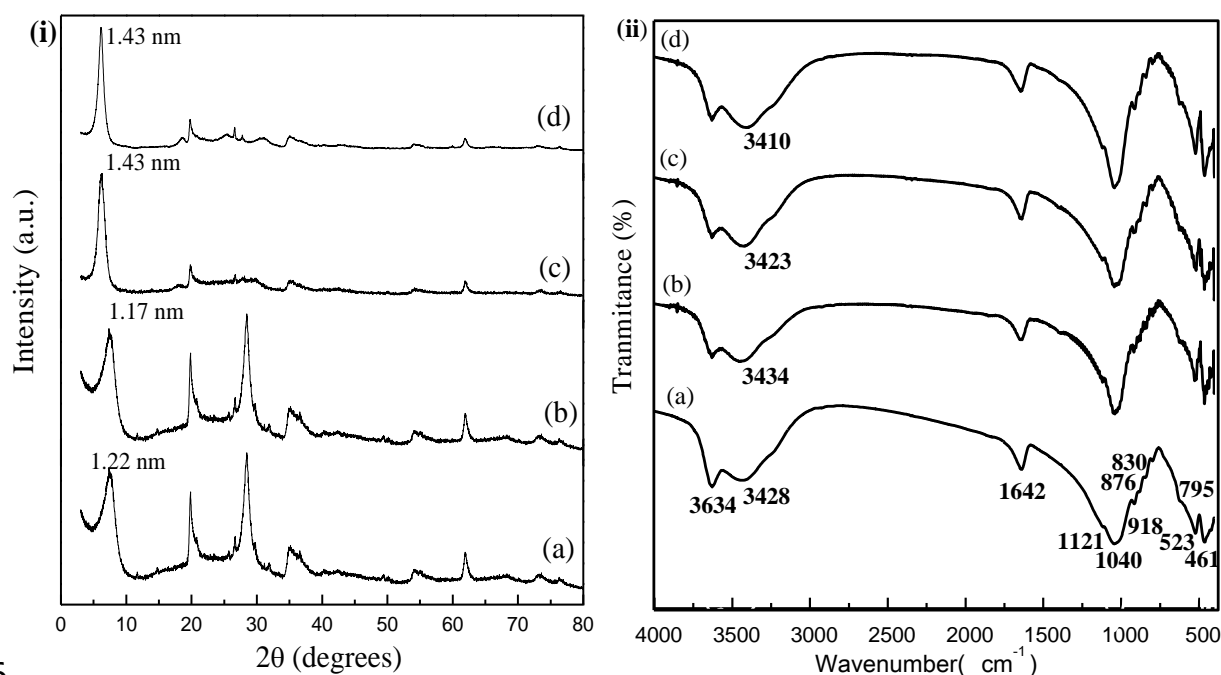


Figure 1 i) XRD patterns and ii) FTIR spectra for (a) Bent, (b) BentNa, (c) BentCa and (d) BentMg.

In the DTG curves for BentNa, BentCa and BentMg (Figure SM2), two mass losses were observed: at 298-660 K and at 660-1200 K for BentNa.. The first is related to the loss of physically adsorbed water and interlayer water, and the second is the result of the dehydroxilation and loss of the coordination water. In the instance of the magnesium and calcium bentonites, three mass losses were observed, at 298-573, 573-754 K and 754-1200 K for BentCa, and at 298-483 K, 483-748 K and 748-1200 K for BentMg. As above, the first loss is related to the loss of adsorbed and interlayer waters, and the second and third ones can be assigned to the dehydroxilation and loss of coordination water, respectively. [30,37]

3.2 Sorption of thiabendazole

The effect of pH on thiabendazole sorption onto BentNa, BentCa and BentMg (Figure 2), showed a maximum sorption of 114 mg g^{-1} for all pH values. Therefore, the value of 1.4 was used in all experiments. The thiabendazole molecules are present at 92 % for TBZ^{++} species ($\text{pK}_a = 2.5$) and 99.9 % for TBZ^+ ($\text{pK}_a = 4.7$). The sorption of thiabendazole is usually pH-dependent [26]. For protonated TBZ (TBZ^+), the sorption onto bentonite occurred by ion exchange between the inorganic cation in the interlayer space and the organic one, TBZ^+ [38].

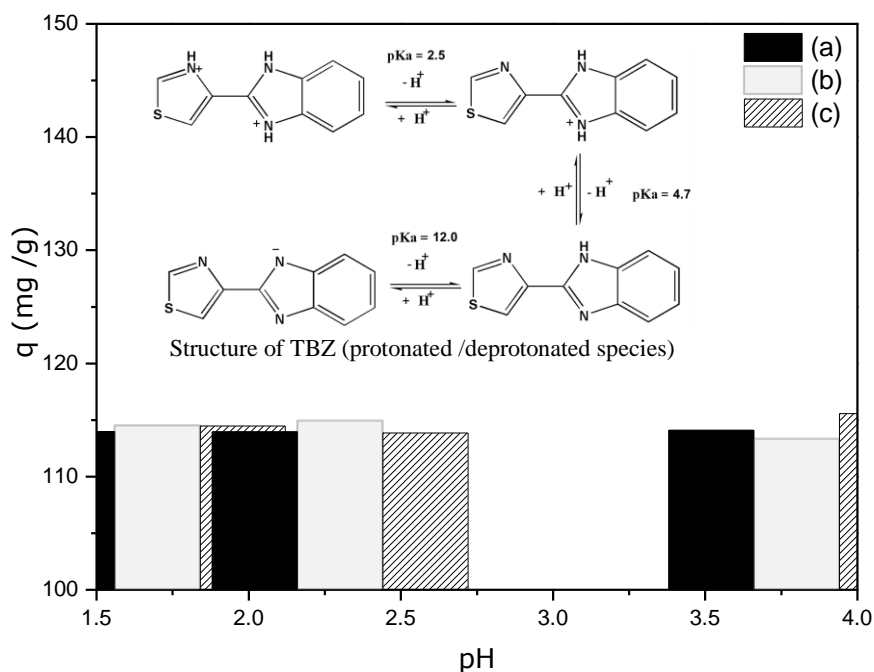


Figure 2. The effect of pH on thiabendazole adsorption onto (a) BentNa, (b) BentCa and (c) BentMg at 300 K. Inserted figure is that of the TBZ structure.

The influence of contact-time on sorption of thiabendazole onto bentonites (Figure 3i), displayed equilibrium at 30, 90 and 75 min where the maximum sorption capacities were 115.5; 111.5 and 111.6 mg g⁻¹ for BentNa, BentCa and BentMg respectively. The data were fitted to second order kinetics (Figure SM3 and Table 1).

The equilibrium isotherms (Figure 3ii) show that the maximum adsorbed quantities are observed at a 2000 mg L⁻¹ for Na-Bent with 185 mg g⁻¹ of Thiabendazole, while for CaBent and Mg-Bent 163 mg g⁻¹ were adsorbed from a starting concentration of 1300 mg L⁻¹. The experimental data were better fitting to the Langmuir than the Freundlich model (Figures SM4.1 and SM4.2), and the resulting parameters are presented in Table 1.

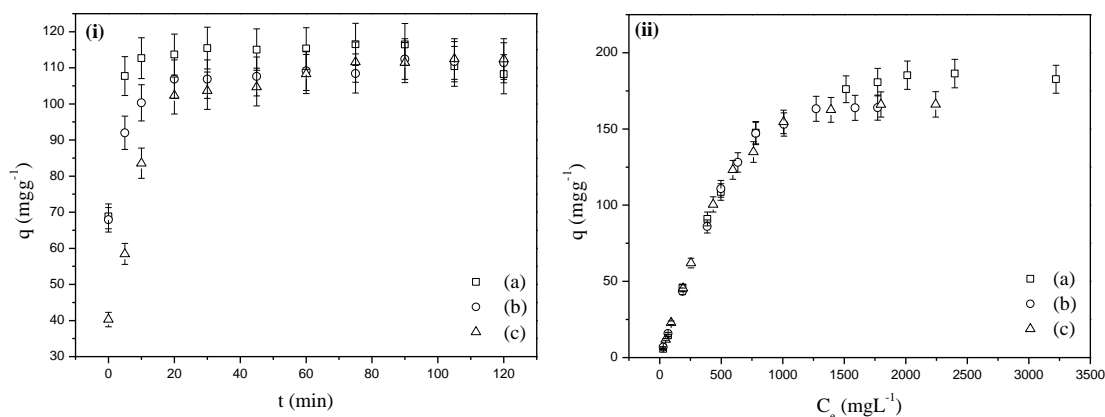


Figure 3. i) Effect of time and ii) initial drug concentration on thiabendazole adsorption on (a) BentNa (b) BentCa and (c) BentMg at 300 K and pH 1.4.

3.3 Characterization of thiabendazole/bentonite hybrids

CHN elemental analysis gave the following results: 164.4; 152.3 and 133.3 mg g⁻¹ of the drug on BentNaTBZ, BentCaTBZ and BentMgTBZ, respectively. XRD patterns (Figure SM5) showed basal spacings altered from 1.17 nm to 1.42 nm in BentNaTBZ, 1.52 nm to 1.41 nm in BentCaTBZ, and 1.43 nm to 1.39 nm in BentMgTBZ. In other words, while for the sodium sample the basal spacing had a higher value, the values decreased for the other two samples, suggesting some loss of water in the intercalation of the organic molecule.

TEM micrographs (Figure 4, Figure SM6) suggested the typical layered arrangement of pristine bentonites with interlayer spacings of 1.15-1.23 nm for BentNa; 1.44-1.56 nm for BentCa and 1.41-1.49 for BentMg. The solids saturated with the drug presented a similar morphology [31,39] and the interplanar spacings were 1.31-1.47 nm for BentNaTBZ, BentCaTBZ and BentMgTBZ, this data in agreement with the XRD patterns (Figure 4).

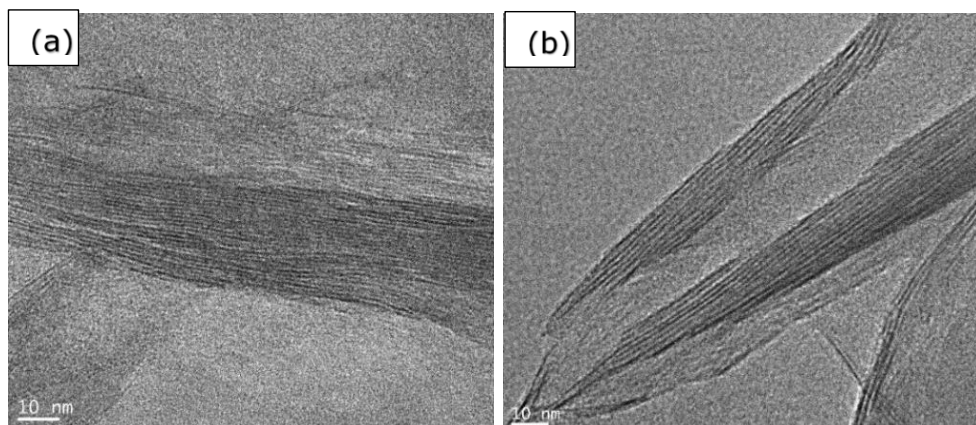


Figure 4. TEM micrographs of (a) BentNa and (b) BentNaTBZ

Taking into consideration the size of thiabendazole (1.15 nm x 0.72 nm x 0.34 nm) [25], the thickness of the montmorillonite (1.35 nm) [30] the XRD patterns and TEM images, the interaction of thiabendazole and bentonite can be seen to be in preponderance through an ion exchange mechanism, involving also the intercalation of the protonated drug in the inter-layer spacing of montmorillonite [26,27].

The FTIR spectra of the hybrids presents typical bands of the free drug (Figure SM7). However, the bands assigned to C-N and N-H have shifted from 1306 to 1313 cm^{-1} possibly as a result of the protonation of the nitrogen of the benzimidazole group, and from 1574 to 1603 cm^{-1} , suggesting the presence of the TBZ^+ and TBZ^{++} forms on the bentonite [27, 40].

UV-VIS spectra for the exchanged samples BentNa, BentCa and BentMg (Figura SM8) displayed a broadadsorption at 250-300 nm, assigned to O \rightarrow Si and O \rightarrow Al charge transfer bands [41]. After drug loading, a band centred at 298 nm was detected and this was the same as that observed for the free drug, which is associated to the n- π and π - π^* molecular orbitals of the TBZ.

3.4 Release test

The release of thiabendazole from hybrids at the solid/liquid interface involved a number of processes which promote the transport of the drug from the solid to the liquid phase. Specifically, for clay minerals, diffusion is relevant and includes drug desorption from the external surface, and the loss of the intercalated molecules from the interlayer region [18].

The release curves for thiabendazole from the three samples over a period of 72 h in the simulated fluids (Figure 5), indicate a similar behavior with a release of 20, 27 and 17 % in the first 9 h for BentNaTBZ; 14, 21 and 27 % for BentCaTBZ and 18, 34 and 32 % for BentMgTBZ SGF, SIF and SBF fluids, respectively. The slow and controlled release is associated to cationic exchange between the intercalated charged drug and the alkaline cations from the simulated fluids [42]

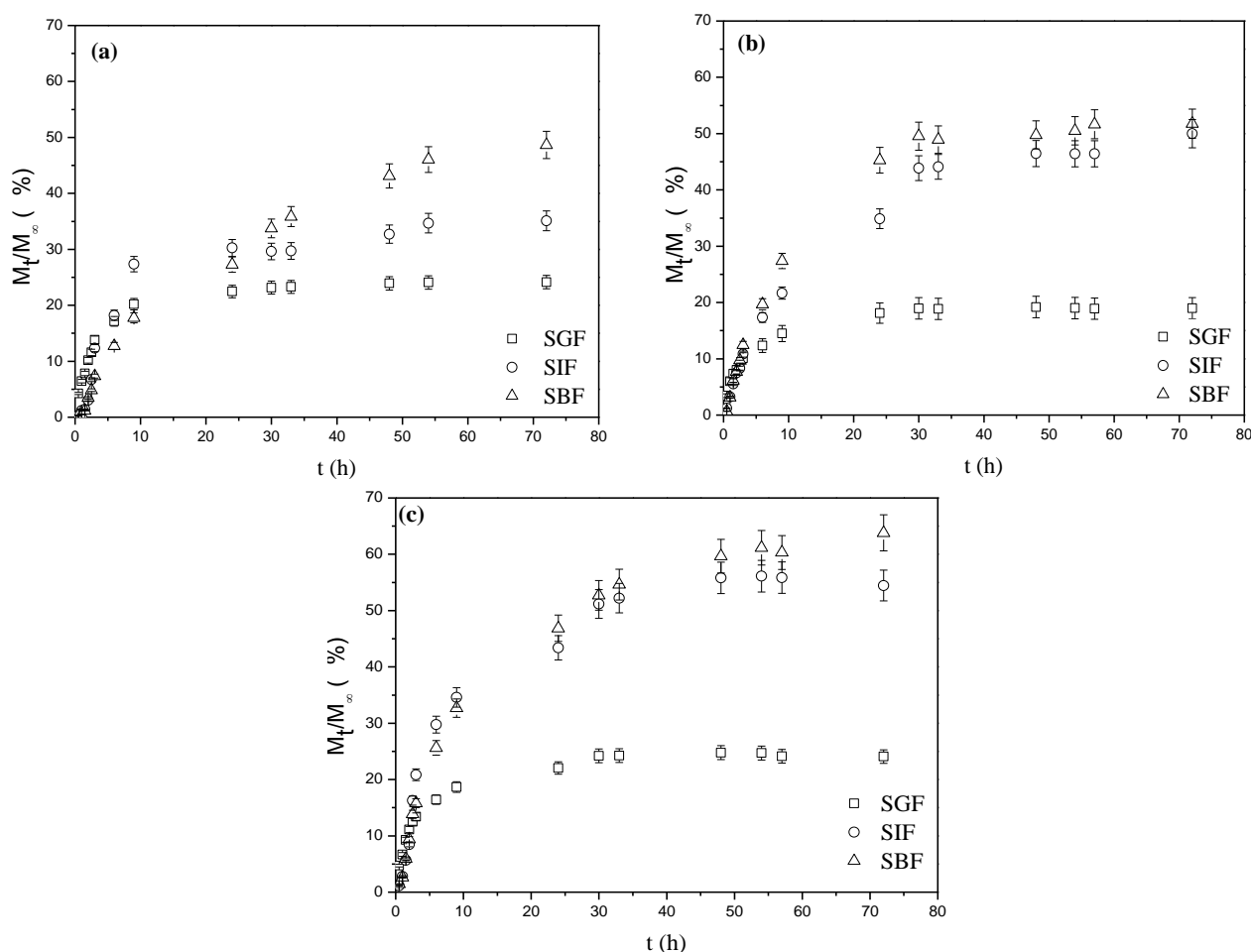


Figure 5. Cumulative release profiles of (a) BentNaTBZ, (b) BentCaTBZ and (c) BentMgTBZ

The quantity of released TBZ species was 100% lower, probably as a result of an equilibrium process in the ion exchange which is a complete reaction [42]. Furthermore, electrostatic interaction between the cations and the anionic charge of the montmorillonite results in incomplete release [43].

The release data were adjusted to Korsmeyer-Peppas model (Equation 3),

$$\frac{M_t}{M_\infty} = kt^n \quad (3)$$

Where M_t/M_∞ is the fractional release of the drug at time t , and k and n kinetic constants. The n value is used to characterize the principal mechanism of drug release; where release is Fickian diffusion when $n \leq 0.45$, if $0.45 \leq n \leq 0.89$, it indicates anomalous (non-Fickian) transport, if $n = 0.89$ the release follows case II and $n > 0.89$ super case II transport [44]

The obtained kinetic parameters (Figure SM9) for the system under investigation are presented in Table 2.

The values of R^2 indicate a good adjustment of the data for BentMgTBZ and BentCaTBZ in the three simulated fluids. The n values were in the range of $0.45 < n < 0.89$ for the release in SGF in all systems, indicating that diffusion and erosion were the main mechanisms at play in the kinetic process of release. It is important to note that this model was proposed for polymers, and therefore the erosion cannot be considered reasonable for a clay mineral matrix [46]

For the TBZ release SIF and SBF, the values of n were 0.89 suggesting that the kinetics of the reaction are based on a super case II transport mechanism, where the diffusion rate of the solvent is higher than the relaxation rate, and the drug release mechanism occurs as a result of swelling and stresses [47].

The XRD patterns of the solids after the release test (Figure SM10) showed that the basal spacings were lower than the initial values observed for the loaded samples: ie. 1.42 nm for Bent Na, 1.41 nm for BentCa, and 1.39 nm for BentMg, suggesting the presence of the unreleased drug in the final solids.

316

317 4. Conclusion

Thiabendazole was loaded onto three exchanged bentonites at different conditions of equilibrium for 45 min and at an initial drug concentration of 2000 mgL^{-1} for BentNa, and for 105 min at an initial drug concentration of 1300 mgL^{-1} for BentCa and BentMg.

The loaded solids behaved as good drug *in vitro* release systems in simulated fluids, with SBF having the highest release of the three samples. The BentMgTBZ

system exhibited the highest cumulative release compared with the other samples. The thiabendazole release kinetics of the drug/bentonite hybrids were similar, and adjusted to the Korsmeyer-Peppas model.

The different tests demonstrated that the nature of the interlayer cation in bentonite influenced the thiabendazole loading and release quantities, and that it is a key parameter that should be considered in the application of bentonites as vehicles for drugs.

Acknowledgments

CNPq is acknowledged for research fellowships to M.G. Fonseca and E.C. Silva Filho. G.R.S. Cavalcanti thanks to CAPES for providing research fellowship. CAPES/COFECUB (835/2015) for financial support.

References

1. Abrahams P. W. Involuntary Soil ingestion and geophagia: a source and sink of mineral nutrients and potentially harmful elements to consumers of earth materials. *Applied Geochemistry*, 2012, 27,954–968.
2. Ghadiri. M., Chrzanowski. W., Rohanizadeh. R. Biomedical applications of cationic clay minerals. *Royal Society of Chemistry*, 2015, 5, 37, 29467–29481.
3. Bergaya. F. Lagaly. G. General Introduction: Clays. *Clay Minerals and Clay Science*. In: Bergaya. F. Theng. B. K. G. Lagaly. G. Eds., *Handbook of Clay Science*. Elsevier. Amsterdam. *Developments in clay science*, 2013, 5,1-19.
4. Brigatti. M. F., Galán. E., Theng. B. K. G. Structure and mineralogy of clay minerals. In: Bergaya. F. Theng. B. K. G. Lagaly. G. Eds., *Handbook of clay science*. Elsevier. Amsterdam. *Developments in clay science*, 2013, 5,21-81.
5. Tangaraj, V.et al., Adsorption and phytophysical properties of fluorescent dyes over montmorillonite and saponite modified by surfactant, *Chemosphere*, 2017, 184, 1355-1361.

6. Jaber, M. et al. Selectivities in adsorption and peptidic condensation in the (arginine and glutamic acid)/montmorillonite clay system, *J. The Journal of Physical Chemistry C*, 2014, 118 (44), 25447–25455.
7. He, H. et al. Silylation of clay mineral surfaces. *Applied Clay Science*, 2013, 71, 15–20.
8. Fournier, F. et al. Physico-chemical characterization of lake pigments based on montmorillonite and carminic acid, *Applied Clay Science*, 2016, 130, 12-17.
9. Gomes, S.S. et al. Silylation of leached-vermiculites following reaction with imidazole and copper sorption behaviour, *Journal of hazardous materials*, 2016, 306, 406-418.
10. Trigueiro, P. et al. Going through wine fining : intimate dialogue between organics and clays, under revision, *Colloids and surfaces b : biointerfaces*, 2018, 166, 1 2018, 79-88.
11. Zhuang, G. et al. Enhancing the rheological properties and thermal stability of oil-based drilling fluids by the synergetic use of organo-montmorillonite and organo-sepiolite, 2018, *Applied Clay Science*, 2018, 161, 505-512.
12. Guillermin, D. et al. New Pigments Based On Carminic Acid And Smectites, A Molecular Investigation, *Pigments And Dyes*, 2019, 160, 971-982.
13. Trigueiro, P. et al. Intimate dialogue between anthraquinone dyes and pillared clay minerals, *Pigments and dyes*, 2018, 159, 384-394.
14. Zhuang, L. et al. Comparative study on the structures and properties of organo-montmorillonite and organo-palygorskite in oil-based drilling fluids, *Journal of industrial and chemical engineering*, 2017, 56, 248-257.

15. Pereira, F. A.R., et al. Green biosorbent based on chitosan-montmorillonite beads for anionic dyes removal, *Journal of Environmental Chemical Engineering*, 2017, 4(5), 3309-3318.
16. El Adraa, K. et al. Montmorillonite-cysteine composites for heavy metal cation complexation: a combined experimental and theoretical study, *Chemical Engeneering Journal*, 2017, 314, 406-417.
17. Rodrigues. L. A. De S. et al. The Systems containing clays and clay minerals from modified drug release: a review. *Colloids and Surfaces B: Biointerfaces*, 2013, 103,642–651.
18. Viseras. C. et al. Current challenges in clay minerals for drug delivery. *Applied Clay Science*, 2010, 48,3, 291–295.
19. Bouaziz, Z. et al. dual role of layered double hydroxide nanocomposites on antibacterial activity and degradation of tetracycline and oxytetracyline, *Chemosphere*, 2018, 2016, 175-183.
20. Shen. J. et al. Mucoadhesive effect of thiolated peg stearate and its modified nlc for ocular drug delivery. *Journal of Controlled Release*, 2010, 137, 217-223.
21. Ruiz- Hitzky. E., Aranda. P., Darder. M. Hybrid and biohybrid materials based on layered clays. In: Brunet. E., Colón. J. L., Clearfield A. Eds. *Tailored Organic-Inorganic Materials*, Wiley, 2015, 245-297.
22. Yang. J. H. et al. Drug-Clay nanohybrids as sustained delivery systems. *Applied Clay Science*, 2016, 130, 20-32.
23. Roca Jalil. M. E. et al. Improvement in the adsorption of thiabendazole by using aluminum pillared clays. *Applied Clay Science*, 2013, 71, 55–63.
24. Roca Jalil, M. E. et al. Effect of the al/clay ratio on the thiabendazol removal by aluminum pillared clays. *Applied Clay Science*, 2014, 87, 245–253.

- 399 25. Yasser Z. E-N. Development of controlled release formulations of thiabendazole
400 Journal of Agricultural Chemistry and Environment,2014,3,1-8.
- 401 26. Lombardi. B., Baschini. M., Torres Sánchez. R. M. Optimization of parameters
402 and adsorption mechanism of thiabendazole fungicide by a montmorillonite of
403 north Patagonia. Applied Clay Science, 2003, 24, 1–2, 43–50.
- 404 27. Lombardi. B. M. et al. Interaction of thiabendazole and benzimidazole with
405 montmorillonite. Applied Clay Science,2006, 33, 1, 59–65.
- 406 28. Xu, W. et al. Controllable release of ibuprofen from size-adjustable and surface
407 hydrophobic mesoporous silica spheres. Powder Technology, 2009,191,1–2, 13–
408 20.
- 409 29. Joshi, G. V. et al. Montmorillonite as a drug delivery system: intercalation and
410 in vitro release of timolol maleate. International Journal of Pharmaceutics,374,
411 1–2, 53–57, 2009a.
- 412 30. Lagaly, G., Ogawa, M., Dékány, I. Clay Mineral-Organic. Em: Bergaya, F.,
413 Theng, B. K. G., Lagaly, G., Eds., Handbook of Clay Science. Elsevier,
414 Amsterdam. Developments In: Clay Science, 2013,5, 435-505.
- 415 31. Sun. Z. et al. XRD, TEM and Thermal analysis of Arizona ca-montmorillonites
416 modified with didodecyldimethylammonium bromide. Journal of Colloid and
417 Interface Science, 2013, 408,1,75–81.
- 418 32. Paz, S. P. A., Angélica, R. S., De Freitas Neves, R. Mg-bentonite in the
419 parnaíba paleozoic basin, northern Brazil. Clays and Clay Minerals, 2012,
420 60,3,265–277.
- 421 33. Madejová. J. FTIR Techniques in clay mineral studies. Vibrational
422 Spectroscopy, 2003,31, 1,1–10.

- 423 34. Tyagi. B., Chudasama. C. D., Jasra. R. V. Determination of structural
424 modification in acid activated montmorillonite clay by FT-IR spectroscopy.
425 Spectrochimica Acta - Part A: Molecular and Biomolecular Spectroscopy,2006,
426 64,2,273–278.
- 427 35. Wu, L. M. et al. Fourier Transform Infrared spectroscopy analysis for
428 hydrothermal transformation of microcrystalline cellulose on montmorillonite.
429 Applied Clay Science,2014, 95,74–82.
- 430 36. Petit. S., Madejova J. Fourier Transform Infrared Spectroscopy. In: Bergaya. F.
431 Theng. B. K. G. Lagaly. G. Eds., Handbook of Clay Science. Elsevier.
432 Amsterdam. Developments in Clay Science, 2013, 5,213-231.
- 433 37. Földvári. M. Handbook of The Thermogravimetric system of minerals and its
434 use in geological practice. Central European Geology, 2011,56, 1-179.
- 435 38. Roca Jalil. E. Desarrollo de arcillas pilareadas con al a partir de una bentonita
436 natural de la norpatagonia argentina para la remoción de tiabendazol. Msc.
437 Thesis. Universidad Nacional De San Luis. San Luis. Argentina. 2010.
- 438 39. Park. Y., Ayoko. G. A., Frost. R. L. Characterisation of organoclays and
439 adsorption of p-nitrophenol: environmental application. Journal of Colloid and
440 Interface Science,2011,360, 2,440–456.
- 441 40. Lin-Vien. Daimay. et al. The Handbook of Infrared and Raman characteristic
442 frequencies of organic molecules. Academic Press,1991. San Diego.
- 443
- 444 41. Zaki, M. I. et al. Ceria on silica and alumina catalysts: dispersion and surface
445 acid- base properties as probed by x-ray diffractometry, UV-Vis diffuse
446 reflectance and in situ IRadsorption studies. Colloids and Surfaces A:
447 Physicochemical and Engineering Aspects,1997,127, 1–3, 47–56.

42. Joshi, G. V. et al. Montmorillonite intercalated with vitamin B1 as drug carrier. Applied Clay Science, 2009b,45, 4,248–253.
43. Nunes, C.D.et al. Load- Ing and delivery of sertraline using inorganic micro and mesoporous materials. European Journal Pharmaceutics Biopharmaceutics, 2007,66,357–365.
44. Mhlana, N., Ray, S. S. Kinetic models for the release of the anticancer drug doxorubicin from biodegradable polylactide/metal oxide-based hybrids. International Journal of Biological Macromolecules, 2015,72,1301–1307.
45. Golubeva, O. Y., Pavlova, S. V., Yakovlev, A. V. Adsorption and in vitro release of vitamin b1 by synthetic nanoclays with montmorillonite structure. Applied Clay Science, 2015,112–113,10–16.
46. Peppas, N.A., Bures, P., Leobandung, W., Ichikawa, H. Hydrogels in pharmaceutical formulations. European Journal Pharm. Biopharm,200,50, 27–46.
47. Munday, D.L, Cox, P.J. Compressed xanthan and karaya gum matrices: hydration, erosion and drug release mechanisms. International Journal of Pharmaceutics,2000,2031-2,179-192.
48. Tımsek. F., Avci. Ö. Investigation of kinetics and isotherm models for the acid orange 95 adsorption from aqueous solution onto natural minerals. Journal of Chemical and Engineering Data,2013,58,3,551–559.